JOURNAL OF NATURAL PRODUCTS

pubs.acs.org/jnp

Article

Drophiobiolins A and B, Bioactive Ophiobolan Sestertepenoids Produced by *Dreschslera gigantea*

Roukia Zatout,[#] Marco Masi,[#] Felicia Sangermano, Maurizio Vurro, Maria Chiara Zonno, Ernesto Santoro, Viola Calabrò, Stefano Superchi, and Antonio Evidente*

Cite This: *J. Nat. Prod.* 2020, 83, 3387−3396

Read Online

ACCESS | Metrics & More | Article Recommendations | Supporting Information

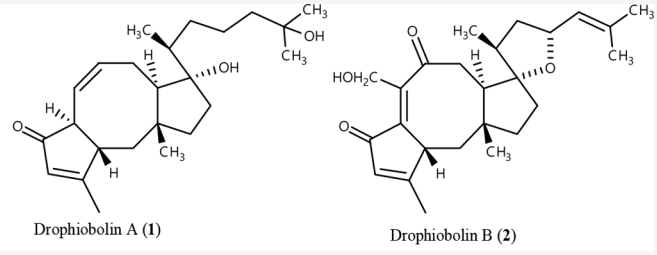

ABSTRACT: Two new bioactive ophiobolan sestertepenoids, named drophiobiolins A and B (**1** and **2**) were isolated from *Drechslera gigantea*, a fungus proposed as a mycoherbicide for biocontrol of *Digitaria sanguinalis*. They were isolated together with ophiobolin A, the main metabolite, 6-*epi*-ophiobolin A, 3-anhydro-6-*epi*-ophiobolin A, and ophiobolin I. Drophiobolins A and B were characterized by NMR, HRESIMS, and chemical methods as 7-hydroxy-7-(6-hydroxy-6-methylheptan-2-yl)-1,9a-dimethyl-3-oxo-3,3a,6,6a,7,8,9,9a,10,10a-decahydrodicyclopenta [*a*,*d*][8]annulene-4-carbaldehyde and 6-(hydroxymethyl)-3′,9,10a-trimethyl-5′-(2-methylprop-1-en-1-yl)-3a,4,4′,5′,10,10a-hexahydro-1*H*,3′*H*-spiro[dicyclopenta[*a*,*d*] [8]annulene-3,2′-furan]-5,7(2*H*,9a*H*)-dione. The relative configuration of drophiobolins A and B, which did not afford crystals suitable for X-ray analysis, was determined by NOESY experiments, while the absolute configuration was assigned by comparison of their experimental and TDDFT calculated electronic circular dichroism (ECD) spectra. The phytotoxic activity of drophiobolins A and B was tested by leaf-puncture assay on cultivated (*Lycopersicon esculentum* L.), as well as on host (*Digitaria sanguinalis* L.) and nonhost (*Chenopodium album* L.) weed plants, compared to that of ophiobolin A. Both of the newly identified ophiobolins showed significant phytotoxicity. Drophiobolins A and B exhibited cytotoxicity against Hela B cells with an IC_{50} value of 10 μM. However, they had a lesser or no effect against Hacat, H1299, and A431 cells when compared to that of ophiobolin A.

Ophiobolins are carbotricyclic sesterterpenoids, well-known naturally occurring compounds. Sesterterpenoids are produced by fungi and marine organisms and are grouped on the basis of their carbon skeleton, which is generated from different arrangements of the acyclic biosynthetic precursor geranylfarnesyl pyrophosphate. Ophiobolene, which is the precursor of all ophiobolins, contains the typical 5-8-5 tricyclic carbon skeleton.[1] This 5-8-5 tricyclic system is shared with the diterpenoid fusicoccin A, the main phytotoxin produced by *Fusicoccum amygdali*[2] and with cotylenins produced by some species of *Cladosporium* sp.[3] Around the same time that Ballio et al. (1968)[2] worked on fusiccocin A and its natural analogues,[4] Canonica et al. (1966)[5,6] and Nozoe et al. (1966)[7] worked on the isolation and characterization of ophiobolin A (**3**), the main phytotoxin produced by the rice pathogen *Helminthosporium orizae* (also known as *Cochliobolus orizae*, or *Drechslera orizae*, or *Bipolaris orizae*).[5−7] Ophiobolin A is the first reported member of the ophiobolan group of metabolites, and several related biologically active ophiobolins were isolated from various fungi, as reviewed by Au et al. (2000),[8] and more recently by Masi et al. (2019).[9] In addition to those previously cited, other ophiobolins were characterized as 14,15-dehydro-6-*epi*-ophiobolin K, 14,15-dehydroophiobolin K, 14,15-dehydro-6-*epi*-ophiobolin G, 14,15-dehydro-ophiobolin G, and 14,15-dehydro-(*Z*)-14-ophiobolin G, isolated from the marine fungus *Aspergillus flocculosus*,[10] bipolaricins A−I isolated from a phytopathogenic *Bipolaris* sp.,[11] asperophiobolins A−K isolated from the mangrove endophytic fungus *Aspergillus* sp. ZJ-68,[12] bipolarolides A−G isolated from *Bipolaris* sp. TJ403-B1,[13] bipolarins A−H isolated from *Bipolaris* sp. TJ403-B1,[14] and maydispenoids A and B, isolated from the phytopathogenic *Bipolaris maydis*.[15] Evidente et al. (2006)[16] reported the isolation of the potential bioherbicide, ophiobolin A (**3**), a sesquiterpenoid produced by

Received: July 27, 2020
Published: October 19, 2020

https://dx.doi.org/10.1021/acs.jnatprod.0c00836
J. Nat. Prod. 2020, 83, 3387−3396

Chart 1

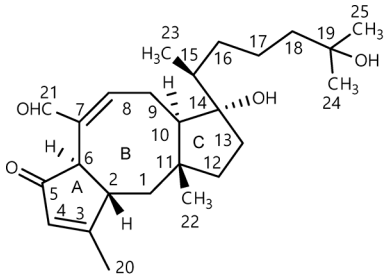

Drophiobolin A (**1**)

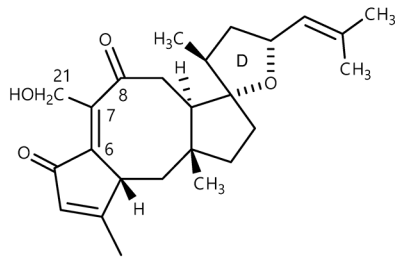

Drophiobolin B (**2**)

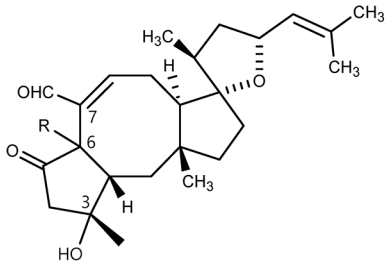

Ophiobolin A (**3**), R=βH
6-*epi*-Ophiobolin A (**4**), R=αH

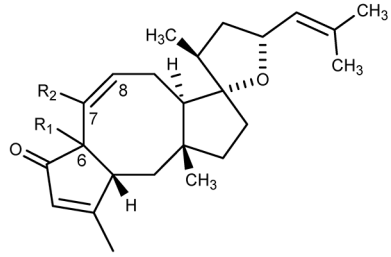

3-Anhydro-6-*epi*-ophiobolin A (**5**), R_1=αH, R_2=CHO
Ophiobolin I (**6**), R_1=βH, R_2=CH_2OH

Drechslera gigantea, a fungus proposed as a mycoherbicide for the control of the weed *Digitaria sanguinalis*.[17] Ophiobolin A (**3**) was shown to be the main phytotoxic metabolite and was isolated together with its congeners, 6-*epi*-ophiobolin A (**4**), 3-anhydro-6-*epi*-ophiobolin A (**5**), and ophiobolin I (**6**).

When assayed on several dicotyledon weeds, ophiobolin A (**3**) showed to be the most phytotoxic among the tested compounds, and the hydroxy group at C-3, the stereochemistry at C-6, and the aldehyde group at C-7 appeared to be important structural features to impart this phytotoxicity.[16] The tridimensional structure of ophiobolin A (**3**), which is closely related to its biological activity, was determined by X-ray diffratometric analysis.[18] Later, ophiobolins E and 8-*epi*-J were isolated from the same culture filtrates together with the known ophiobolins B and J thatshowed phytotoxic activity when tested on some weeds.[19]

On the basis of the biological activity reported by Au et al. (2000),[8] ophiobolin A (**3**) was assayed for its growth-inhibitory activity in both plant and mammalian cells inducing cell death in *Nicotiana tabacum* L. cv. Bright Yellow 2 (TBY-2) cells, showing typical features of apoptosis-like cell death, and inhibited the growth of eight cancer cell lines by 50% after 3 days. Ophiobolin A also showed significant antitumor activity on the B16F10 mouse melanoma model with lung pseudometastases when assayed at 10 mg/kg (IC_{50} 0.29 ± 0.05 μM)[20] and inhibited the proliferation and migration of glioblastoma multiforme (GBM) cells, probably by inhibition of the Ca^{2+}-activated K^+ channel (BKCa) channel activity at big conductance. The results obtained in this study also suggested that **3** induced paraptosis-like cell death in GBM cells, which correlated with the cytoplasmatic vacuolization, possibly brought about by the swelling and fusion of mitochondria and/or the endoplasmic reticulum (ER).[21] These results prompted to increase the efficacy of **3** by its formulation in nanoparticles. These chemoembolization particles were synthesized for its delivery and tested to investigate the cell death mechanism on a rhabdomyosarcoma cancer (RD), which is the most common soft tissue sarcoma in children. The use of **3** onto RD cells in culture showed a 70% reduction in cells.[22]

All the results obtained on the cytotoxic activity of **3** and its congener have been recently reviewed.[9] After we considered the very promising cytotoxic activity of ophiobolin A, its total synthesis was also recently realized in 14 steps.[23]

The study in progress on the cytotoxic activity of ophiobolin A and particularly on its mode of action required its constant and continued production by fermentation using *D. gigantea*. From an in depth investigation of the mother liquors of **3** crystallization and of the other fractions obtanined during the purification steps, two new ophiobolins were isolated and named drophiobolins A and B (**1** and **2**).

This manuscript then reports the chemical and the biological characterization of drophiobolins A and B (**1** and **2**) as well as their absolute configuration (AC) assignment.

RESULTS AND DISCUSSION

The organic extract obtained from the culture filtrates of *D. gigantea* was purified, as detailed in the Experimental Section, obtaining two new ophiobolan sesterterpenoids, drophiobolins A and B (**1** and **2**), ophiobolin A, 6-*epi*-ophiobolin A, 3-anhydro-6-*epi*-ophiobolin A, and ophiobolin I (**3**–**6**) (Figure 1).

The well-known ophiobolins (**3**–**6**) were identified by comparing their spectroscopic data (^{1}H NMR and ESIMS) and the phisical properties with reported data.[16]

The preliminary ^{1}H and ^{13}C NMR investigation showed that drophiobolin A (**1**) was related to 3-anydro-6-*epi*-ophiobolin A (**5**),[24,25] while drophiobolins B (**2**) appeared to be related to ophiobolin I (**6**).[16]

A molecular formula of $C_{25}H_{38}O_4$ for drophiobolin A (**1**) was deduced from its HRESIMS spectrum, which is consistent with seven indices of hydrogen deficiency. The comparison of

https://dx.doi.org/10.1021/acs.jnatprod.0c00836
J. Nat. Prod. 2020, 83, 3387−3396

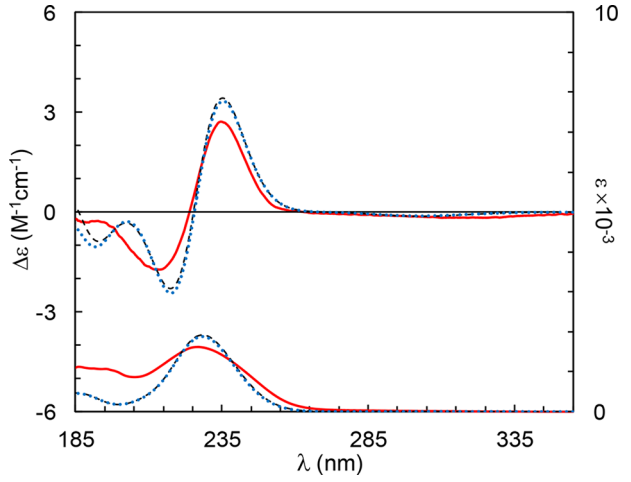

Figure 1. Comparison between experimental (solid red line) and calculated (TDDFT/CAM-B3LYP/6-311++G(2d,2p)/IEFPCM-(acetonitrile) ECD and UV spectra for (2*S*,6*R*,10*R*,11*R*,14*S*,15*S*)-**1a** (dashed black lines) and (2*S*,6*R*,10*R*,11*R*,14R,15*S*)-**1b** (dotted blue lines).

its ^{1}H and ^{13}C NMR spectra with those of 3-anhydro-6-*epi*-ophiobolin A (**5**)[24,25] confirmed their structural relationship. These findings were confirmed by the bands typical for the hydroxy, carbonyl, and olefinic groups and the absorption maxima for an extended conjugated system recorded in the IR[26] and UV[27] spectra, respectively.

In particular, the ^{1}H and COSY[28] data (Table 1) showed the presence of a singlet, a double doublet (J = 6.3 and 2.4 Hz), and a broad singlet due to the protons of an aldehydic (H-21) and two trisubstituted olefinic (H-8 and H-4) groups at δ 9.33, 6.82, and 6.05, respectively.

H-8 coupled with the hydrogens of the adjacent methylene group (H_2C-9) which resonate both as a multiplet at δ 2.70 and 2.09 and these, in turn, with the broad double doublet (J = 14.0 and 2.8 Hz) of the adjacent methine hydrogen (H-10) at δ 2.57. H-9A overlapped the multiplet of an allylic hydrogen (H-2) resonating as multiplet at δ 2.70 which coupled with the two multiplets of the hydrogens of adjacent methylene group (H_2C-1) observed at δ 2.12 and 1.34. These signals accounted for the hydrogen of a suitable pentasubstituted fusacyclocte-nefuranone system. The multiplets of the hydrogens of two adjacent methylene groups (H_2C-12 and H_2C-13) of the 1,1,2,3,3-pentasubstituted cyclopentane were observed at δ 2.01 and 1.44 and 1.55 and 1.33, while the singlet and the broad singlet of tertiary (Me-22) and a vinyl methyl (Me-20) groups resonated at δ 0.89 and 2.08, respectively.

Furthermore, the same two spectra also showed the signals of a 1,5-dimethyl-5-hydroxyhexyl side chain which was located

Table 1. NMR Data of Drophiobolins A and B (1 and 2)[a,b]

	1			2		
no.	δ_C[c]	δ_H (J in Hz)	HMBC	δ_C[c]	δ_H (J in Hz)	HMBC
1	46.5 t	2.12 m	H_3-22	48.2 t	1.94 dd (13.9 and 2.1)	H-2, H_3-22
		1.34 m			1.28 m[e]	
2	49.2 d	2.70 m[f]	H-6, H-10, H_3-20	44.6 d	3.07 br d (11.9)	H_3-20
3	177.8 s		H-1B, H_3-20	177.3 s		H-2, H_3-20
4	130.7 d	6.05 br s	H_3-20	131.8 s	6.10 br s	H_3-20
5	207.5 s		H-6	197.2 s		H-4, H_3-20
6	50.2 d	3.47 d (4.2)	H-21	135.5 s		H-4
7	141.1 s		H-6, H-21	146.9 s		H_2-9, H_2-21
8	155.9 d	6.82 dd (6.3, 2.4)	H-6, H_2-9	210.5 s		
9	31.9 t	2.70 m[f]	H-8	42.8 t	2.60 dd (14.0 and 3.3)	H-10
		2.09 m			2.50 t (14.0)	
10	54.9 d	2.57 br dd (14.0, 2.8)	H-8, H_3-22	51.2 d	2.86 dd (14.0 and 3.3)	H_2-9, H-15, H_3-22
11	45.2 s		H_2-1, H_2-12, H_3-22	43.1 s		H_3-22
12	41.8 t	2.01 m, 1.44 m[f]	H_2-13, H_3-22,	29.8 t	1.59 m, 1.28 m[e]	H_2-13
13	23.3 t	1.55 m[f], 1.33 m	H-12B	41.4 t	1.70 m (2H)	H_3-23
14	88.8 s		H-15, H_3-23	95.5 s		H_2-9, H-10, H_3-23
15	38.2 d	1.44 m[f]	H_3-23	36.4 d	2.11 m[e]	H_2-16, H_3-23
16	33.5 t	1.14 m, 1.12 m	H_3-23	41.8 t	1.76 q (7.8), 1.73 m	H-15, H_3-23
17	35.7 t	1.55 m[f], 1.44 m[f]	H-15	72.0 d	4.60 q (7.8)	
18	44.6 t	1.55 m[f], 1.44 m[f]	H_3-24, H_3-25	126.8 d	5.20 d hept (7.8 and 1.2)	H_3-25
19	71.4 s		H_3-24, H_3-25	135.0 s		H_3-24, H_3-25
20	17.7 q	2.08 br s	H-4, H-6	17.4 q	2.11 br s[e]	H-4
21	193.3 d	9.33 s	H-6, H-8	59.3 t	4.89 dd (14.8 and 4.0)	
					4.44 dd (14.8 and 7.8)	
22	23.0 q	0.89 s	H-13B	20.9 q	0.97 s	H_2-12
23	15.5 q	0.97 d (6.7)		16.1 q	1.05 d (7.8)	H-15, H_2-16
24[d]	29.8 q[f]	1.26 br s[f]		25.9 q	1.73 d (1.2)	H-18, H_3-25
25[d]	29.8 q[f]	1.26 br s[f]		18.1 q	1.68 d (1.2)	H-18, H_3-24
OH					3.63 br dd (7.8, 4.0)	

[a] ^{1}H (2D), ^{1}H (COSY), and ^{13}C and ^{1}H (HSQC) NMR experiments confirmed the correlations of all the protons and the corresponding carbons. [b] Coupling constants (J) are given in parentheses. [c] Multiplicities were assigned with DEPT. [d] These signals could be exchanged. [e] These signals are in part overlapped. [f] These signals overlapped.

https://dx.doi.org/10.1021/acs.jnatprod.0c00836
J. Nat. Prod. 2020, 83, 3387−3396

at the tertiary hydroxylated carbon (C-14) of the cyclopentane on the basis of the long-range couplings observed in the HMBC[28] spectrum (Table 1) between C-14 with H-15 and Me-23, which resonated as a multiplet and a doublet (J = 6.7) at δ 1.44 and 0.97, respectively.

H-15 coupled with the two hydrogens of the adjacent methylene groups (H_2C-16) at δ 1.44 and 1.12, with the hydrogens of the adjacent methylene group (H_2C-17) at δ 1.55 and 1.44, which overlapped the multiplets of the residual methylene group (H_2C-18). Finally, the two tail methyl groups Me-24 and Me-25 gave one only overlapped singlet at δ 1.26.[27] The couplings observed in the HSQC[28] spectrum (Table 1) allowed the chemical shifts to be assigned to the protonated carbons of the ^{13}C NMR spectrum. Consequently, the signals observed at δ 155.9, 130.7, 54.9, 50.2, 49.2, 46.5, 44.6, 41.8, 38.2, 35.7, 33.5, 29.8, 23.3, 23.0, 17.7, and 15.5 in the ^{13}C NMR spectrum were assigned to C-8, C-4, C-10, C-6, C-2, C-1, C-18, C-12, C-15, C-17, C-16, C-24 and C-25 (overlapped signals), C-13, C-22, C-20, and C-23, respectively.[29] The residual six carbons (one typical of a carbonyl group, two olefinic carbons, and three sp^3 carbons) were also assigned on the basis of the long-range couplings observed in the HMBC spectrum. In particular, the coupling between the signals at δ 207.5 with H-6, 177.8 with H-1B and Me-20, 141.1 with H-6 and H-21, 88.8 with H-15 and Me-23, 71.4 with Me-24 and Me-25, and 45.2 with H_2-1, H_2-12, and Me-22 allowed for them to be assigned to C-5, C-3, C-7, C-14, C-19, and C-11. Thus, the chemical shifts to all the carbons and corresponding hydrogens of **1** were assigned and reported in Table 1. These data appeared consistent with the typical ophiobolan 5-8-5 fused ring system, and **1** was formulated as 7-hydroxy-7-(6-hydroxy-6-methylheptan-2-yl)-1,9a-dimethyl-3-oxo-3,3a,6,6a,7,8,9,9a,10,10a-decahydrodicyclopenta [*a*,*d*][8]-annulene-4-carbaldehyde.

The structure assigned to **1** was supported by the other correlations observed in the HMBC spectrum and by the data from its HRESIMS spectrum which showed the presence of a trimeric sodium adduct $[3\ M + Na]^+$, the protonated dimeric $[2\ M + H]^+$, and sodium $[M + Na]^+$ and protonated $[M + H]^+$ adduct ions at m/z 1229, 805, 425, and 403.2858, respectively. The latter, by two consecutive losses of water, generated the significant fragmentation ions $[M + H - H_2O]^+$ and $[M + H - 2 \times H_2O]^+$, at m/z 385 and 367.

Drophiobolin B (**2**) has a molecular formula of $C_{25}H_{34}O_4$, as deduced from its HRESIMS spectrum, and it is consistent with nine indices of hydrogen deficiency. Its ^{1}H NMR and COSY data (Table 1) showed the presence of a broad singlet and a double heptet (J = 7.8 and 3.3 Hz) at δ 6.10 and 5.20 due to the olefinic hydrogens H-4 and H-18 being later coupled with the quartet (J = 7.8 Hz) of the adjacent hydroxylated methine hydrogen (H-17) observed at δ 4.60 and also allylic coupled with the terminal methyl groups of the side chain (Me-24 and Me-25).[22] H-17 coupled with only one hydrogen of the adjacent methylene group (CH_2-16) which resonates as a quartet (J = 7.8 Hz) at δ 1.76, while the other appeared as a multiplet at δ 1.73. These latter protons (H_2-16) coupled with the adjacent methine hydrogen (H-15) resonating as a multiplet at δ 2.11, in part overlapped to the signal of a vinyl methyl group (Me-20) present as a broad singlet at δ 2.11. H-15 also coupled with the hydrogens of the adjacent methyl group (Me-23), and was observed as a doublet (J = 7.8 Hz) at δ 1.05. In the same spectra, a broad singlet and two doublets (J = 1.2 Hz) of the other three vinyl methyl groups (Me-20 and Me-24 and Me-25) were observed at δ 2.11 and 1.73 and 1.68, respectively. The signals of the AB part of an ABX system corresponding to the hydrohylated methylene group HO−CH_2-21 were observed as two double doublets (J = 14.8 and 4.0 Hz and J = 14.8 and 7.8 Hz) at δ 4.89 and 4.44, which were coupled with the germinal hydroxy group, the X part, appearing as a broad double doublet (J = 7.8 and 4.0 Hz) at δ 3.63. A double doublet (J = 14.4 and 3.3 Hz) and a triplet (J = 14.4 Hz) for the hydrogens of a methylene group (H_2C-9) α-located to the carbonyl group (O═C-8) were observed at δ 2.60 and 2.50 and coupled with a methine hydrogen (H-10), which, being α-located to an oxygentad tertiary carbon, resonated as a double doublet (J = 14.4 and 3.3 Hz) at δ 2.86. In addition, a broad doublet (J = 11.9 Hz) of an allylic methine hydrogen (H-2) was observed at δ 3.07 and coupled with the hydrogens of the adjacent methylene group (CH_2-1) resonating as a double doublet (J = 13.9 and 2.1 Hz) and a multiplet at δ 1.94 and 1.28, with the latter in part overlapped with the signal of one of the hydrogens of CH_2-12. The allylic coupling (<1 Hz) between H-2 and Me-20 was also observed.[27] Finally, the singlet of a tertiary methyl group (Me-22) and the multiplets of the hydrogens accounted for two coupled methylene groups (CH_2-13 and CH_2-12) of a pentasubstituted cyclopentane and were observed at δ 0.97, 1.70 (2H), and 1.59 and 1.28, respectively. These findings, the absence of the protons H-6 and H-8, and that significant of the aldehydic hydrogen, confirmed that **2** is close to ophiobolin I,[31] but this differed for the isomerization of the double bond of the octacyclic B ring from C-7−C-8 to C-7−C-6 and the presence of a carbonyl group at C-8.

Thus, the structure of a $\Delta^{6,7}$-8,*O*-dehydro ophiobolin I could be suggested for drophiobolin B, which was confirmed by the typical band for hydroxy, carbonyl, and olefinic groups and the absorption maxima for an extended conjugated system observed in its IR[26] and UV[27] spectra, respectively.

The ^{13}C NMR data (Table 1) showed, as expected, the presence of the signals for 25 carbons, and the correlations recorded in the HSQC spectrum (Table 1) allowed for the signals of the protonated carbons to be assigned. In particular, the signals at δ 131.8, 126.8, 72.0, 59.3, 51.2, 48.2, 44.6, 42.8, 41.8, 41.4, 36.4, 29.8, 25.9, 20.9, 18.1, 17.4, and 16.1 were assigned to C-4, C-18, C-17, C-21, C-10, C-1, C-2, C-9, C-16, C-13, C-15, C-12, C-24, C-22, C-25, C-20, and C-23, respectively.[29] The four sp^2 and the two sp^3 carbons, one of which is oxygenated, were assigned by the long-range couplings observed in the HMBC spectrum (Table 1). In particular, the coupling between the signal at δ 177.3 with H-2 and Me-20; 146.9 with H_2-9 and H_2-21; 135.5 with H-4; 135.0 with Me-24 and Me-25; 95.5 with H_2-9, H-10, and Me-23; and 43.1 with Me-22 allowed for them to be assigned to C-3, C-7, C-6, C-19, C-14, and C-11, respectively. Finally, the signals of the two carbonyls at δ 210.5 and 197.2 were assigned to C-8 and C-5 for the couplings observed in the HMBC spectrum between C-5 with H-4 and Me-20.[24]

Thus, the chemical shifts to all hydrogens and corresponding carbons were attributed and reported in Table 1, and drophiobolin B (**2**) was formulated as 6-(hydroxymethyl)-3′,9,10a-trimethyl-5′-(2-methylprop-1-en-1-yl)-3a,4,4′,5′,10,10a-hexahydro-1*H*,3′*H*-spiro[dicyclopenta[*a*,*d*][8]annulene-3,2′-furan]-5,7(2*H*,9a*H*)-dione.

The structure assigned to **2** was supported by the other correlations observed in the HMBC spectrum and by the data from its HRESIMS spectrum which showed the dimeric

https://dx.doi.org/10.1021/acs.jnatprod.0c00836
J. Nat. Prod. 2020, 83, 3387−3396

sodium $[2\ M + Na]^+$, the protonated dimeric $[2\ M + H]^+$ adducts, and the protonated $[M + H]^+$ ions at m/z 819, 797, and 399.2526. The latter, by loss of water, generated the significant fragmentation $[M + H - H_2O]^+$ ion at m/z 381.

The relative configuration of drophiobolins A and B (**1** and **2**) was deduced from the correlations observed in the corresponding NOESY spectra.[28]

NOESY spectrum of **1** (Table 2) showed the correlation between H-2 and Me-22 and H-6 with H-10, while there were

Table 2. NOESY Data of Drophiobolin A (1)

irradiated	observed	irradiated	observed
H-21	H-8	H_2-9	H-8
H-8	H_2-9	H_3-22	H-2
H-4	H_3-20	H_3-20	H-4
H-6	H-10		

no observed correlations between H-6 with H-2 and H-10 with Me-22. Thus, H-2 and Me-22 were located on the same side of the molecule, and H-6 and H-10 were located on the opposite side. This indicates a *trans*-junction between A and B and B and C rings.[12]

However, such NOESY analysis did not allow to assign the relative configuration to C-15 and C-14, because due to the rotational freedom of the side chain attached to C-14, compound **1** lacks the significant correlation observed in **2**. Such a side chain comes from a reductive opening of the tetrahydrofuran D ring, also previously observed in ophiobolin B.[5,6,9,19]

In the NOESY data of **2** (Table 3) significant correlations between H-2 and Me-22, H-10 with H-15, and H-17 and Me-

Table 3. NOESY Data of Drophiobolin B (2)

irradiated	observed	irradiated	observed
H-2	H_3-22, H_3-20	H-18	H_3-24
H-10	H-15, H_2-9	H-17	H_3-23, H-16B
H-21A	H-21B, OH	H-4	H_3-20

23 were observed, while H-10 did not correlated with Me-22. These results indicated that H-2, Me-22, Me-23, and H-17 were on the same side of the molecule, and H-10 and H-15, as well as the ether bridge of the tetrahydrofuran D ring, were on the opposite side. Thus, the B/C ring junction is *trans*, as in **1**.

The absolute configuration of drophiobolins A and B (**1** and **2**) was assigned by comparison of the experimental and TDDFT computed electronic circular dichroism (ECD) spectra,[30] following a particularly reliable and straightforward approach for the absolute configuration assignment in solution to chiral complex natural compounds.[31,32] Accordingly, the UV and ECD spectra of **1** were recorded in acetonitrile in the 180−360 nm range (Figure 1).

The UV spectrum displays an intense broad band at 227 nm allied to the absorption of the two α,β-unsaturated carbonyl moieties present on the molecule, while the ECD spectrum displays an intense coupletlike feature centered at 224 nm and constituted by a positive Cotton effect (CE) at 235 nm ($\Delta\varepsilon$ 2.75) and a negative one at 214 nm ($\Delta\varepsilon$ −1.69), followed by a broad weak CE at about 290 nm ($\Delta\varepsilon$ −0.07). The ECD couplet can be interpreted as allied to an exciton coupling effect[33] between the $\pi-\pi^*$ transitions of the two α,β-unsaturated carbonyl chromopheres, i.e., the cyclopentenone and the exocyclic unsaturated aldehyde moieties, while the CE at 290 nm can be ascribed to an overlap of their $n-\pi^*$ carbonyl transitions. Computational conformational analysis of **1** was then carried out, taking into account the (2*S**,6*R**,10*R**,11*R**) relative configuration of the A/B/C tricyclic system established by NMR (*vide supra*). On the contrary, NMR analysis did not provide the relative configuration at C-14 and C-15. Therefore, the computational analysis was carried out on both epimers at C-14, while the absolute configuration at C-15, being undeterminable by ECD analysis, was assumed to be (*S*), as observed in all the reported ophioboline-type molecules.[12,34] In this case, partial knowledge of the relative configuration permits avoidance of carrying out computations on all diastereomers[35] limiting the investigation to the two epimers at C-14. The conformational analysis was first carried out at the molecular mechanics (MM) level on the chosen theoretical models (2*S*,6*R*,10*R*,11*R*,14*S*,15*S*)-**1a** and (2*S*,6*R*,10*R*,11*R*,14*R*,15*S*)-**1b**. The conformers found were then further optimized by density functional theory (DFT) at the DFT/B3LYP/TZVP/IFPCM(acetonitrile) level of theory, taking into account the solvation effect by the IFPCM approach.[36] Computations provided eight and five appreciably populated conformers for **1a** and **1b**, respectively (see Table S1, Table S2, Figure S15, and Figure S16 in the Supporting Information). The conformers essentially differed by the conformation of the side chain, the tricyclic moiety being quite rigid. Moreover, as inferred from Figure 2, in both

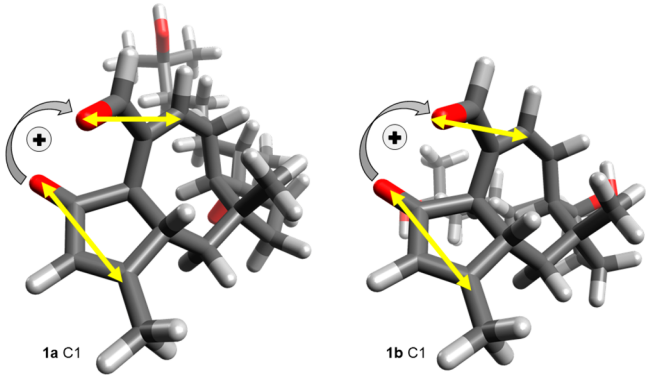

Figure 2. Most stable conformers of epimers **1a** and **1b** indicating the exciton chirality defined by electric transition allied to the two α,β-unsaturated carbonyl chromophores.

1a and **1b**, the $\pi-\pi^*$ electronic transitions allied to the cyclopentenone and the α,β-unsaturated aldehyde chromophores define a positive chirality which, according to the Harada−Nakanishi exciton chirality rule,[37] predicts a positive couplet feature in the ECD spectrum, as experimentally observed[38] (see Figure S18, Figure S19, and the detailed dicussion in the Supporting Information). This supports the preliminary assignment of the 2*S*,6*R* absolute configuration to the stereocenters of the A/B bycyclic system, and by combining this information with the relative stereochemistry assigned by NMR to C-10 and C-11, we can assign the absolute configuration to these stereocenters as 10*R*,11*R*. This stereochemical assignment was further confirmed in a more rigorous way by TDDFT computations.

UV and ECD spectra for both **1a** and **1b** epimers were calculated on previously found conformers at the TDDFT/CAM-B3LYP/6-311++G(2d,2p)/IFPCM(acetonitrile) level of

https://dx.doi.org/10.1021/acs.jnatprod.0c00836
J. Nat. Prod. 2020, 83, 3387−3396

theory and Boltzmann averaged over conformer populations. As inferred from Figure 1, the UV and ECD spectra of **1a** and **1b** are almost superimposable and do not allow a reliable assignment of the AC at C-14. Thus, neither NMR nor ECD analysis helps the assignment of the correct stereochemistry at this stereocenter. However, we assume that the side chain at C-14 is β, as it is in all the ophibolin-type compounds known so far,[9,12,34] and therefore that the absolute configuration at that stereocenter is (*S*). The comparison between the ECD experimental spectrum for **1** and those computed for **1a** and **1b** (Figure 1) shows agreement for all three main spectral features observed. In particular, the sign and shape of the coupletlike feature centered at 224 nm and of the broad weak carbonyl band at 290 nm are very well-reproduced. Therefore, the (2*S*,6*R*,10*R*,11*R*,14*S*,15*S*) AC can be reliably assigned to the isolated drophobiolin A (**1**).

The AC of drophobiolins B (**2**) was then assigned following the same approach. Accordingly, the UV and ECD spectra of **2** were recorded in the 180−360 nm range in acetonitrile (Figure 3).

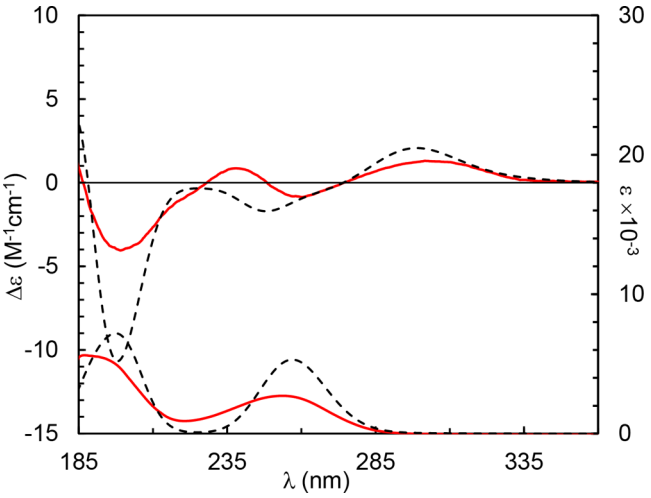

Figure 3. Comparison between experimental (solid red line) and calculated (TDDFT/CAM-B3LYP/6-311++G(2d,2p)/IEFPCM-(acetonitrile)) ECD and UV spectra for compound (2*R*,10*R*,11*R*,14*S*,15*S*,17*R*)-**2** (dashed black lines).

The UV spectrum displays two intense broad bands at 254 nm and ca. 190 nm allied to the two α,β-unsaturated carbonyl chromophores. The ECD spectrum displays four, alternate in sign, main CEs at 302 nm ($\Delta\varepsilon$ +1.30), 360 nm ($\Delta\varepsilon$ −0.85), 238 nm ($\Delta\varepsilon$ +0.85), and 199 nm ($\Delta\varepsilon$ −4.04), respectively. In this case, the NMR analysis provided the relative configuration of all the sterocenters (*vide supra*); therefore, the computational conformational analysis could be carried out on the single (2*R*,10*R*,11*R*,14*S*,15*S*,17*R*)-**2** steroisomer, taking into account the known (2*R**,10*R**,11*R**,14*S**,15*S**,17*R**) relative configuration. After a first optimization at the MM level, the found conformers were refined at the DFT/B3LYP/TZVP/IFPCM(acetonitrile) level of theory, obtaining seven appreciably populated conformers (see Table S3 and Figure S17, in the Supporting Information). Again, the tetracyclic A/B/C/D system appeared to be quite rigid, with the main conformational differences due to rotation of the unsaturated side chain on C-17. The UV and ECD spectra for (2*R*,10*R*,11*R*,14*S*,15*S*,17*R*)-**2** were then calculated on previously found conformers at the TDDFT/CAM-B3LYP/6-311++G(2d,2p)/IFPCM(acetonitrile) level of theory and Boltzmann averaged over conformer populations. As inferred from Figure 3, the computed UV and ECD spectra are in very good agreement with the experimental ones, and the main ECD bands are reproduced in sign, wavelength position, and intensity. The (2*R*,10*R*,11*R*,14*S*,15*S*,17*R*) absolute configuration, chosen for the calculation, can be then assigned to the isolated drophobiolin B (**2**).

The structure of **2** was disclosed while the present article was ready for submission; it was a metabolite, named maydispenoids B from *Bipolaris maydis*, collected from *Anoectochilus roxburghii* (Wall.) and found during a screening for immunosuppressive compounds from fungi.[15]

The phytotoxic activity of the drophiobolins A and B, compared to that of ophiobolin A, was tested by leaf-puncture assay on the host weed plant (*Digitaria sanguinalis* L.), nonhost weed (*Chenopodium album* L.), and cultivated (*Lycopersicon esculentum* L.) plants. When tested at 10^{-3} M (Table 4, Figure

Table 4. Phytotoxic Activity of Drophiobolins A and B (1 and 2) Compared to that of Ophiobolin A (3)[a]

	1		2		3		control[b]
	10^{-3}[c]	10^{-4}	10^{-3}	10^{-4}	10^{-3}	10^{-4}	
Digitaria sanguinalis L.	3	2	3	2	3	3	0
Lycopersicon esculentum L.	3	2	3	2	3	3	0
Chenopodium album L.	1	0	2	1	3	2	0

[a]Observations were made 2 days after treatment. Diameter of necrosis on leaves: 3, necrosis >3 mm; 2, necrosis between 2 and 3 mm; 1, necrosis between 1 and 2 mm; 0, no necrosis. [b]MeOH (2%) in distilled water. [c]Molar concentration.

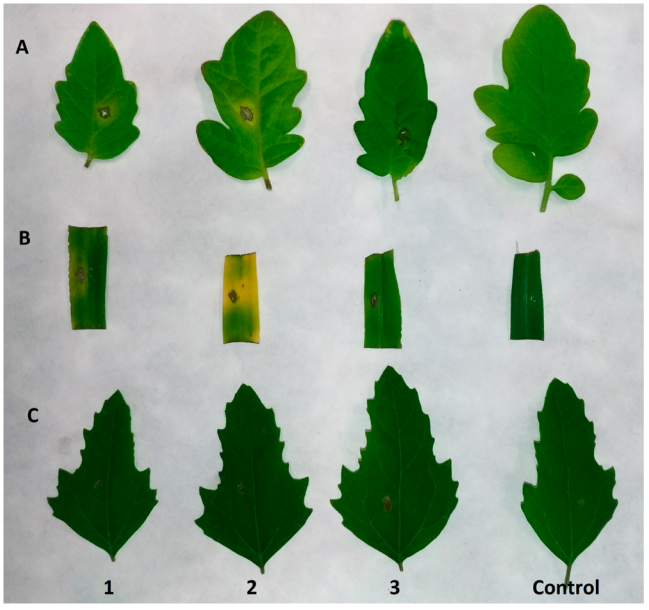

Figure 4. Phytotoxic activity induced by drophiobolins A and B (**1** and **2**) and ophiobolin A (**3**) when tested at 10^{-3} M by leaf-puncture assay on cultivated plant ((A) *Lycopersicon esculentum* L.) and on weeds ((B) *Digitaria sanguinalis* L. and (C) *Chenopodium album* L.); control is 2% MeOH in distilled water.

https://dx.doi.org/10.1021/acs.jnatprod.0c00836
J. Nat. Prod. 2020, 83, 3387−3396

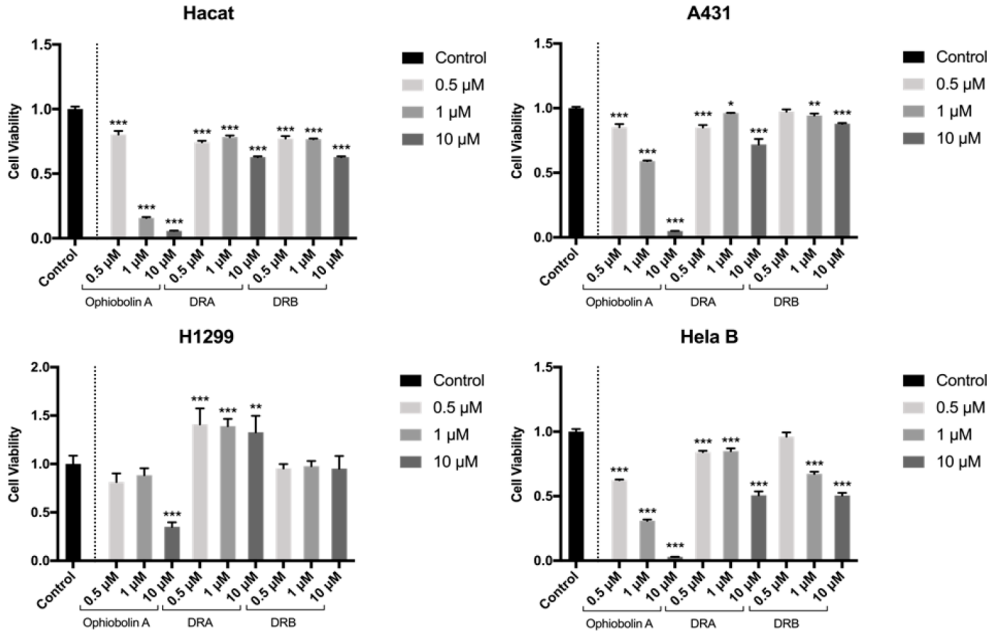

Figure 5. Effects of drophiobolins A or B (DRA and DRB) on cell viability. MTT assays of Hacat, Hela, A431, and H1299 cells incubated for 24 h with 0.5, 1, and 10 μM drophiobolins A or B were compared with that of ophiobolin A. Data are expressed as absorbance and presented as mean ± SD of three independent experiments, each done in triplicate. Analysis of variance was performed by one-way Anova and multiple comparisons. *P < 0.5 when compared with the control.

4), both **1** and **2** showed the same phytotoxicity as that of ophiobolin A on the host plant and tomato. Lower toxicity was observed on *C. album* with respect to **3**. At 10^{-4} M, the toxicity of **1** and **2** slightly decreases on all tested plants with **1** being inactive on *C. album*.

The evaluation of the *in vitro* cytotoxicity was performed in A431, Hela B, and H1299 cancer cells as well as in Hacat immortalized keratinocytes. The experiments with the new ophiobolins, drophiobolins A and B, were performed in parallel with those of the already described ophiobolin A. After 24 h of treatment, increasing amounts (from 0.5 to 10 μM) of **1** or **2** slightly reduced cell viability of Hacat (up to 63%) and A431 (up to 72%), while Hela cell viability was significantly reduced (up to 50%, IC_{50} 10 μM), as shown in Figure 5 and Table S4. Ophiobolin A, instead, had dramatic effects on these cell lines (Figure 5). H1299 had a very different behavior when it was stimulated by drophiobolin A at all concentrations tested, while drophiobolin B was ineffective.

Interestingly, ophiobolin A, which was previously demonstrated to be cytotoxic against glioblastoma,[39] appeared to be almost ineffective on H1299 lung cancer cells thus showing tumor-cell specificity.

EXPERIMENTAL SECTION

General Experimental Procedures. Optical rotations of MeOH solutions were measured using a Jasco P-1010 digital polarimeter; IR spectra of glassy films were recorded on a PerkinElmer Spectrum One FT-IR spectrometer. UV and ECD spectra were recorded at room temperature on a JASCO J815 spectropolarimeter, using 0.5 mm cells and concentrations of about 4.5×10^{-3} M for **1** and 2.5×10^{-3} M for **2**. ^{1}H and ^{13}C NMR spectra were recorded at 400 and 100 MHz, respectively, in $CDCl_3$ on a Bruker spectrometer. The same solvent was used as an internal standard. Carbon multiplicities were determined by DEPT spectra.[28] DEPT, COSY-45, HSQC, HMBC, and NOESY experiments[28] were performed using Bruker microprograms. HRESI and ESI mass spectra and liquid chromatography (LC)/MS analyses were performed using the LC/MS TOF system AGILENT 6230B, HPLC 1260 Infinity. The HPLC separations were performed with a Phenomenex LUNA (C_{18} (2) 5 μ 150 × 4.6 mm). Analytical and preparative TLC was performed on silica gel plates (Merck, Kieselgel 60, F_{254}, 0.25 and 0.5 mm, respectively) or on reverse phase (Whatman, KC18 F_{254}, 0.20 mm) plates; the compounds were visualized by exposure to UV light and/or iodine vapors and/or by spraying first with 10% H_2SO_4 in MeOH, and then with 5% phosphomolybdic acid in EtOH, followed by heating at 110 °C for 10 min. CC = silica gel (Merck, Kieselgel 60, 0.063−0.200 mm).

Fungal Strain. The strain of *Drechslera gigantea* used in this study was isolated during extensive field surveys in Florida from naturally infected large crabgrass (*Digitaria sanguinalis*).[40] It was stored as PDA slants both in the Biological Control of Weeds Collection at the Plant Pathology Department of University of Florida (Gainsville, FL, USA) and Institute of Science and Food Production, CNR, Bari, Italy. *D. gigantea* was grown in a mineral medium liquid, as previously reported in detail.[16]

Production, Extraction, and Purification of the Metabolites. The lyophilized material obtained from the culture filtrates (4 L) was dissolved in distilled water (400 mL, final pH 4.5) and extracted with EtOAc (3 × 400 mL). The organic extracts were combined, dehydrated with Na_2SO_4, filtered, and evaporated under reduced pressure obtaining a brown oil residue (1.2 g), which was fractionated by CC eluted with $CHCl_3$-*iso*-PrOH (96:4) yielding 11 groups of homogeneous fractions. The residue of the third fraction (540.0 mg) was crystallized with EtOAc-*n*-hexane (1:5) giving white crystals of ophiobolin A (**3**, 448.2 mg). The residue obtained from the mother liquors of crystallization (91.8 mg) was further purified by TLC and eluted three times with $CHCl_3$-*iso*-PrOH (98:2), yielding five bands. The first and fifth bands resulted in two homogeneous amorphous solids identified as 3-anhydrous-6-*epi*-ophiobolin A (**5**, 13.2 mg) and 6-*epi*-ophiobolin A (**4**, 7.9 mg). From the second band, a further amount of **4** (24.5 mg) was obtained as a white crystalline solid. The residues of the third (3.4 mg) and fourth (2.6 mg) bands were further purified on TLCs and eluted with *n*-hexane-EtOAc (65:35) and petroleum ether-acetone-EtOAc (75:15:10), yielding an amorphous solid, which is new, as reported below, and was named drophiobolin B (**2**, 1.9 mg). The residue of the seventh fraction (36.0 mg) of the first column was further purified by two successive steps on TLC, using as

https://dx.doi.org/10.1021/acs.jnatprod.0c00836
J. Nat. Prod. 2020, 83, 3387−3396

eluent. The first eluent was EtOAc-*n*-hexane (5.5:4.5), and then it was $CHCl_3$-*iso*-PrOH (94:6), yielding another amorphous solid identified as ophiobolin I (**6**, 8.9 mg). The residue of the ninth fraction was further purified on reverse phase TLC, using acetone-H_2O (75:25) as eluent, and then on TLC eluted with $CHCl_3$-*iso*-PrOH (95:5) yielding another amorphous solid, which being new, as below reported, was named drophiobolin A (**1**, 1.2 mg).

Drophiobolin A (1). This compound is an amorphous solid. IR ν_{max} 3422, 1734, 1615 cm^{-1}. UV λ_{max} nm (log ε) 275 (3.6). For ^1H and ^{13}C NMR data, see Table 1. HR ESIMS (+): *m*/*z* 1229 $[3\ M + Na]^+$, 805 $[2\ M + H]^+$, 425 $[M + Na]^+$, 403.2858 [calcd for $C_{25}H_{39}O_4$ 403.2848 $M + H]^+$, 385 $[M + H - H_2O]^+$, 367 $[M + H - 2xH_2O]^+$.

Drophiobolin B (2). This compound is an amorphous solid. IR ν_{max} 3421, 1737, 1646, 1614 cm^{-1}. UV λ_{max} nm (log ε) 276 (3.6). For ^1H and ^{13}C NMR data, see Table 1. HR ESIMS (+): *m*/*z* 819 $[2\ M + Na]^+$, 797 $[2\ M + H]^+$, 399.2526 [calcd for $C_{25}H_{35}O_4$ 399.2535, $M + H]^+$, 381 $[M + H - H_2O]^+$.

Computational Details. Preliminary conformational analyses were performed by the Spartan02 package[41] employing the MMFF94s molecular mechanics force field with Monte Carlo searching and the arbitrary fixing of ACs (2*S*,6*R*,10*R*,11*R*,14*S*,15*S*) and (2*S*,6*R*,10*R*,11*R*,15*S*,15*S*) for the two epimers **1a** and **1b** of **1** and (2*R*,10*R*,11*R*,14*S*,15*S*,17*R*) for **2**. All possible conformers were searched, considering the degrees of freedom of the system within an energy window of 30 kcal/mol. The minimum energy conformers found by molecular mechanics were further fully optimized by using the DFT at the DFT/B3LYP/TZVP level taking into account the solvent effect by using the IEFPCM implicit model with acetonitrile as solvent, by the Gaussian09 package.[42] All conformers are real minima; no imaginary vibrational frequencies have been found, and the free energy values have been calculated and used to get the Boltzmann population of conformers at 298.15 K. The DFT/B3LYP/TZVP/IEFPCM(acetonitrile) geometries were employed as input geometries for calculation of UV and ECD spectra at the TDDFT/CAM-B3LYP/6-311++G(2d,2p)/IEFPCM(acetonitrile) level of theory. The theoretical UV and ECD spectra were obtained as the average over the conformer Boltzmann populations. The ECD spectra were obtained from calculated excitation energies and rotational strengths, as a sum of Gaussian functions centered at the wavelength of each transition, with a parameter σ (width of the band at 1/2 height) of 0.3 eV. To guarantee origin independence and to evaluate the quality of the molecular wave functions employed, theoretical ECD spectra were obtained both in the length and velocity representation, using the lowest 30 states. The velocity/length calculated spectra were almost coincident, indicating a good level of calculation. Therefore, in all figures, only the velocity-form predicted spectra are reported. Calculated spectra have been red-shifted by 10 nm for compounds **1a** and **1b** and by 12 nm for compound **2**. In addition, the intensity of compounds **1a** and **1b** have been scaled by 30 units, and that of compound **2** has been scaled by 4 units.

Phytotoxic Assay. The phytotoxic activity of drophiobolins A and B and ophiobolin A (**1**-**3**) was tested at 10^{-3} and 10^{-4} M by leaf-puncture assay on weeds (*Digitaria sanguinalis* L. and *Chenopodium album* L) and a cultivated plant (*Lycopersicon esculentum* L.), as previously reported.[11] The compounds were dissolved in MeOH and then diluted to the desired concentration with distilled water (final concentration of MeOH 2%).

Cytotoxic Activity MTT Assay. The effect of drophiobiolins A and B on cell viability was evaluated on human immortalized Hacat skin keratinocytes and tumor-derived A431 (epidermoid carcinoma), H1299 (nonsmall cell lung carcinoma), and HeLa B (cervix adenocarcinoma) cell lines. Drophobiolins A and B cytotoxicities were compared to that of ophiobolin A. Cells were seeded at 10^4 in 96 well plates. Twenty-four hours later, the medium was changed and supplemented with drophobiolins A and B and ophiobolin A (from 0.5 μM to 10 μM) in DMSO. After 24 h of incubation, cell viability was determined by MTT assays. Aliquots (10 μL) of MTT solution 1:10 (stock solution 5 mg/mL) were added to each well containing 100 μL of medium and incubated with cells for 4 h. After incubation, the medium was removed, and 150 μL aliquots of DMSO were added to each well to solubilize the formazan crystals. Optical density was measured after 4 h with an ELISA reader (Bio-Rad) in a dual-wavelength mode (570 and 630 nm) filter using an iMark microplate reader (Bio-Rad) and calculated as follows: absorbance (570 nm) − absorbance (630 nm). The cell viability was calculated as (absorbance of test sample)/(absorbance of control). All experiments were performed in triplicates and presented as mean ± standard deviation calculated using GraphPad Prism8 software. Analysis of variance was performed by one-way Anova and multiple comparisons. $^*P < 0.5$ when compared with the control.

■ ASSOCIATED CONTENT

Supporting Information

The Supporting Information is available free of charge at https://pubs.acs.org/doi/10.1021/acs.jnatprod.0c00836.

^1H and ^{13}C NMR data (1D and 2D) and HRESIMS spectra of **1** and of **2**, experimental and computed ECD spectra, Boltzmann distribution, structures of computed conformers, molecular orbital analysis, and cell viability MTT assay (PDF)

■ AUTHOR INFORMATION

Corresponding Author

Antonio Evidente − *Dipartimento di Scienze Chimiche, Università di Napoli Federico II, 80126 Napoli, Italy;* orcid.org/0000-0001-9110-1656; Phone: +39 081 2539178; Email: evidente@unina.it

Authors

Roukia Zatout − *Dipartimento di Scienze Chimiche, Università di Napoli Federico II, 80126 Napoli, Italy; Laboratoire de Mycologie, de Biotechnologie et de l'Activité Microbienne (LaMyBAM), Département de Biologie Appliquée, Université des Frères Mentouri, 25017 Constantine, Algeria*

Marco Masi − *Dipartimento di Scienze Chimiche, Università di Napoli Federico II, 80126 Napoli, Italy;* orcid.org/0000-0003-0609-8902

Felicia Sangermano − *Dipartimento di Biologia, Università di Napoli Federico II, 80126 Napoli, Italy*

Maurizio Vurro − *Istituto di Scienze delle Produzioni Alimentari, CNR, 70126 Bari, Italy;* orcid.org/0000-0001-6875-4093

Maria Chiara Zonno − *Istituto di Scienze delle Produzioni Alimentari, CNR, 70126 Bari, Italy*

Ernesto Santoro − *Dipartimento di Scienze, Università della Basilicata, 85100 Potenza, Italy*

Viola Calabrò − *Dipartimento di Biologia, Università di Napoli Federico II, 80126 Napoli, Italy*

Stefano Superchi − *Dipartimento di Scienze, Università della Basilicata, 85100 Potenza, Italy;* orcid.org/0000-0002-7265-1625

Complete contact information is available at: https://pubs.acs.org/10.1021/acs.jnatprod.0c00836

Author Contributions

#R.Z. and M.M. equally contributed to this work.

Notes

The authors declare no competing financial interest.

https://dx.doi.org/10.1021/acs.jnatprod.0c00836
J. Nat. Prod. 2020, 83, 3387−3396

■ ACKNOWLEDGMENTS

The authors thank Dr. Raghavan Charudattan, University of Florida, USA, for supplying the isolate of *D. gigantea* and Roberta Di Lecce for her technical contribution to this work.

■ REFERENCES

(1) Dewick, P. M. *Medicinal Natural Products—A Biosynthetic Approach*, 3rd ed.; John Wiley & Sons Ltd: Chichester, 2009, pp 137−234.
(2) Ballio, A.; Brufani, M.; Casinovi, C. G.; Cerrini, S.; Fedeli, W.; Pellicciari, R.; Santurbano, B.; Vaciago, A. *Experientia* **1968**, *24*, 631−635.
(3) Sassa, T.; Ooi, T.; Nukina, M.; Ikeda, M.; Kato, N. *Biosci., Biotechnol., Biochem.* **1998**, *62*, 1815−1818.
(4) Graniti, A. *Experientia* **1991**, *47*, 751−864.
(5) Canonica, L.; Fiecchi, A.; Galli Kienle, M.; Scala, A. *Tetrahedron Lett.* **1966**, *7*, 1211−1218.
(6) Canonica, L.; Fiecchi, A.; Galli Kienle, M.; Scala, A. *Tetrahedron Lett.* **1966**, *7*, 1329−1333.
(7) Nozoe, S.; Hirai, K.; Tsuda, K. *Tetrahedron Lett.* **1966**, *7*, 2211−2216.
(8) Au, T. K.; Chick, W. S. H.; Leung, P. C. *Life Sci.* **2000**, *67*, 733−742.
(9) Masi, M.; Dasari, R.; Evidente, A.; Mathieu, V.; Kornienko, A. *Bioorg. Med. Chem. Lett.* **2019**, *29*, 859−869.
(10) Choi, B. K.; Trinh, P. T. H.; Lee, H. S.; Choi, B. W.; Kang, J. S.; Ngoc, N. T. D.; Van, T. T. T.; Shin, H. J. *Mar. Drugs* **2019**, *17*, 346.
(11) Liu, M.; Sun, W.; Shen, L.; Hao, X.; Al Anbari, W. H.; Lin, S.; Li, H.; Gao, W.; Wang, J.; Hu, Z.; Zhang, Y. *J. Nat. Prod.* **2019**, *82*, 2897−2906.
(12) Cai, R.; Jiang, H.; Mo, Y.; Guo, H.; Li, C.; Long, Y.; Zhang, Z.; She, Z. *J. Nat. Prod.* **2019**, *82*, 2268−2278.
(13) Liu, M.; Sun, W.; Shen, L.; He, Y.; Liu, J.; Wang, J.; Hu, Z.; Zhang, Y. *Angew. Chem.* **2019**, *131*, 12219−12223.
(14) Liu, M.-T.; He, Y.; Shen, L.; Hu, Z.-X.; Zhang, Y.-H. *J. Nat. Medicines* **2019**, *17*, 935−944.
(15) Duan, X.; Tan, X.; Gu, L.; Liu, J.; Hao, X.; Tao, L.; Feng, H.; Cao, Y.; Shi, Z.; Duan, Y.; Deng, M.; Chen, G.; Qi, C.; Zhang, Y. *Bioorg. Chem.* **2020**, *99*, 103816.
(16) Evidente, A.; Andolfi, A.; Cimmino, A.; Vurro, M.; Fracchiolla, M.; Charudattan, R. *J. Agric. Food Chem.* **2006**, *54*, 1779−1783.
(17) Kenfield, D.; Bunkers, G.; Wu, Y. U.; Strobel, G.; Sugawara, F.; Hallock, Y.; Clardy, J. *Experientia* **1989**, *45*, 900−902.
(18) Andolfi, A.; Evidente, A.; Santini, A.; Tuzi, A. *Acta Crystallogr., Sect. E: Struct. Rep. Online* **2006**, *62*, o2195−o2197.
(19) Evidente, A.; Andolfi, A.; Cimmino, A.; Vurro, M.; Fracchiolla, M.; Charudattan, R.; Motta, A. *Phytochemistry* **2006**, *67*, 2281−2287.
(20) Bury, M.; Novo-Uzal, E.; Andolfi, A.; Cimini, S.; Wauthoz, N.; Heffeter, P.; Lallemand, B.; Avolio, F.; Delporte, C.; Cimmino, A.; Dubois, J.; et al. *Int. J. Oncol.* **2013**, *43*, 575−585.
(21) Bury, M.; Girault, A.; Megalizzi, V.; Spiegl-Kreinecker, S.; Mathieu, V.; Berger, W.; Evidente, A.; Kornienko, A.; Gailly, P.; Vandier, C.; Kiss, R. *Cell Death Dis.* **2013**, *4*, e561−e561.
(22) Morrison, R.; Gardiner, C.; Evidente, A.; Kiss, R.; Townley, H. *Pharm. Res.* **2014**, *31*, 2904−2917.
(23) Thach, D. Q.; Brill, Z. G.; Grover, H. K.; Esguerra, K. V.; Thompson, J. K.; Maimone, T.J. *Angew. Chem., Int. Ed.* **2020**, *59*, 1532−1536.
(24) Kim, J. M.; Hyeon, S. B.; Isogai, A.; Suzuki, A. *Agric. Biol. Chem.* **1984**, *48*, 803−805.
(25) Pena-Rodriguez, L. M.; Chilton, W. S. *J. Nat. Prod.* **1989**, *52*, 1170−1172.
(26) Nakanishi, K.; Solomon, P. H. *Infrared Absorption Spectroscopy*, 2nd ed.; Holden Day: Oakland, 1977; pp 17−44.
(27) Pretsch, E.; Bühlmann, P.; Affolter, C. *Structure Determination of Organic Compounds—Tables of Spectral Data*, 3rd ed.; Springer−Verlag: Berlin, 2000; pp 161−243.
(28) Berger, S.; Braun, S. *200 and More Basic NMR Experiments: A Practical Course*, 1st ed.; Wiley−VCH: Weinheim, 2004.
(29) Breitmaier, E.; Voelter, W. *Carbon-13 NMR Spectroscopy*; VCH: Weinheim, 1987; pp 183−280.
(30) Autschbach, J. *Ab initio* electronic circular dichroism and optical rotatory dispersion: from organic molecules to transition metal complexes. In *Comprehensive Chiroptical Spectroscopy*; Berova, N., Polavarapu, P. L., Nakanishi, K., Woody, R. W., Eds.; Vol. *1*; John Wiley & Sons, Inc.: Hoboken, NJ, 2012; pp 593−642.
(31) For recent reviews on application to natural products see: (a) Molinski, T. F.; Morinaka, B. I. *Tetrahedron* **2012**, *68*, 9307−9343. (b) Kong, L.-Y.; Wang, P. *J. Nat. Med.* **2013**, *11*, 193−198. (c) Nugroho, A. E.; Morita, H. *J. Nat. Med.* **2014**, *68*, 1−10. (d) Batista, J. M., Jr; Blanch, E. W.; Bolzani, V. D. S. *Nat. Prod. Rep.* **2015**, *32*, 1280−1302. (e) Superchi, S.; Scafato, P.; Górecki, M.; Pescitelli, G. *Curr. Med. Chem.* **2018**, *25*, 287−320. (f) Mándi, A.; Kurtán, T. *Nat. Prod. Rep.* **2019**, *36*, 889−918.
(32) For recent examples from our group see: (a) Santoro, E.; Messina, F.; Marcotullio, M. C.; Superchi, S. *Tetrahedron* **2014**, *70*, 8033−8039. (b) Evidente, M.; Cimmino, A.; Zonno, C.; Masi, M.; Berestetskiy, A.; Santoro, E.; Superchi, S.; Vurro, M.; Evidente, A. *Phytochemistry* **2015**, *117*, 482−488. (c) Santoro, S.; Superchi, S.; Messina, F.; Santoro, E.; Rosati, O.; Santi, C.; Marcotullio, M. C. *J. Nat. Prod.* **2013**, *76*, 1254−1259. (d) Vergura, S.; Santoro, E.; Masi, M.; Evidente, A.; Scafato, P.; Superchi, S.; Mazzeo, G.; Longhi, G.; Abbate, S. *Fitoterapia* **2018**, *129*, 78−84. (e) Belviso, S.; Santoro, E.; Lelj, F.; Casarini, D.; Villani, C.; Franzini, R.; Superchi, S. *Eur. J. Org. Chem.* **2018**, *2018*, 4029−4037. (f) Santoro, E.; Mazzeo, G.; Petrovic, A. G.; Cimmino, A.; Koshoubu, J.; Evidente, A.; Berova, N.; Superchi, S. *Phytochemistry* **2015**, *116*, 359−366. (g) Evidente, M.; Santoro, E.; Petrovic, A. G.; Cimmino, A.; Koshoubu, J.; Evidente, A.; Berova, N.; Superchi, S. *Phytochemistry* **2016**, *130*, 328−334. (h) Coronado-Aceves, E. W.; Gigliarelli, G.; Garibay-Escobar, A.; Robles Zepeda, R. E.; Curini, M.; López Cervantes, J.; Espitia-Pinzón, C. I.; Superchi, S.; Vergura, S.; Marcotullio, M. C. *J. Ethnopharmacol.* **2017**, *206*, 92−100.
(33) Harada, N.; Nakanishi, K. *Circular Dichroic Spectroscopy—Exciton Coupling in Organic Stereochemistry*; University Science Books: Mill Valley, CA, 1983.
(34) Zhu, T.; Lu, Z.; Fan, J.; Wang, L.; Zhu, G.; Wang, Y.; Li, X.; Hong, K.; Piyachaturawat, P.; Chairoungdua, A.; Zhu, W. *J. Nat. Prod.* **2018**, *81*, 2−9.
(35) Johnson, J. L.; Raghavan, V.; Cimmino, A.; Moeini, A.; Petrovic, A. G.; Santoro, E.; Superchi, S.; Berova, N.; Evidente, A.; Polavarapu, P. L. *Chirality* **2018**, *30*, 1206−1214.
(36) Tomasi, J.; Mennucci, B.; Cammi, R. *Chem. Rev.* **2005**, *105*, 2999−3094.
(37) Harada, N.; Nakanishi, K.; Berova, N. Electronic CD Exciton Chirality Method: Principles and Applications. In *Comprehensive Chiroptical Spectroscopy*; Berova, N., Polavarapu, P. L., Nakanishi, K., Woody, R. W., Eds.; Vol. *2*; John Wiley & Sons, Inc.: Hoboken, NJ, 2012; pp115−166.
(38) For a recent application of the exciton chirality model on enone chromophores see: Pescitelli, G.; Di Bari, L. *Chirality* **2017**, *29*, 476−485.
(39) Dasari, R.; Masi, M.; Lisy, R.; Ferdérin, M.; English, L. R.; Cimmino, A.; Mathieu, V.; Brenner, A. J.; Kuhn, J. G.; Whitten, S. T.; Evidente, A.; Kiss, R.; Kornienko, A. *Bioorg. Med. Chem. Lett.* **2015**, *25*, 4544−4548.
(40) Chandramohan, S.; Charudattan, R. *Biol. Control* **2001**, *22*, 246−255.
(41) *SPARTAN 02*; Wavefunction, Inc.: Irvine, CA.
(42) Frisch, M. J.; Trucks, G. W.; Schlegel, H. B.; Scuseria, G. E.; Robb, M. A.; Cheeseman, J. R.; Scalmani, G.; Barone, V.; Mennucci, B.; Petersson, G. A.; Nakatsuji, H.; Caricato, M.; Li, X.; Hratchian, H. P.; Izmaylov, A. F.; Bloino, J.; Zheng, G.; Sonnenberg, J. L.; Hada, M.; Ehara, M.; Toyota, K.; Fukuda, R.; Hasegawa, J.; Ishida, M.; Nakajima, T.; Honda, Y.; Kitao, O.; Nakai, H.; Vreven, T.; Montgomery, J. A., Jr.; Peralta, J. E.; Ogliaro, F.; Bearpark, M.;

https://dx.doi.org/10.1021/acs.jnatprod.0c00836
J. Nat. Prod. 2020, 83, 3387−3396

Heyd, J. J.; Brothers, E.; Kudin, K. N.; Staroverov, V. N.; Kobayashi, R.; Normand, J.; Raghavachari, K.; Rendell, A.; Burant, J. C.; Iyengar, S. S.; Tomasi, J.; Cossi, M.; Rega, N.; Millam, J. M.; Klene, M.; Knox, J. E.; Cross, J. B.; Bakken, V.; Adamo, C.; Jaramillo, J.; Gomperts, R.; Stratmann, R. E.; Yazyev, O.; Austin, A. J.; Cammi, R.; Pomelli, C.; Ochterski, J. W.; Martin, R. L.; Morokuma, K.; Zakrzewski, V. G.; Voth, G. A.; Salvador, P.; Dannenberg, J. J.; Dapprich, S.; Daniels, A. D.; Farkas, O.; Foresman, J. B.; Ortiz, J. V.; Cioslowski, J.; Fox, D. J. *Gaussian 09*, revision A.02; Gaussian, Inc.: Wallingford, CT, 2009.

https://dx.doi.org/10.1021/acs.jnatprod.0c00836
J. Nat. Prod. 2020, 83, 3387−3396